

## Synthesis and Characterization of the 4,4'-Bipyridyl Dianion and Radical Monoanion. A Structural Study

Mark S. Denning, Mark Irwin, and Jose M. Goicoechea\*

Department of Chemistry, Chemistry Research Laboratory, University of Oxford, Mansfield Road, Oxford OX1 3TA, U.K.

Received April 23, 2008

The reaction of ethylenediamine solutions of 4,4'-bipyridine with varying stoichiometric amounts of sodium resulted in the isolation of the 4,4'-bipyridyl radical anion ( $44\text{bipy}^{\cdot-}$ ) and the unprecedented 4,4'-bipyridyl dianion ( $44\text{bipy}^{2-}$ ). The radical was characterized by single-crystal X-ray diffraction in  $\text{Na}(44\text{bipy})(\text{en})$  (**1**) and  $\text{Na}_2(44\text{bipy})_2(\text{en})_2$  (**2**) and the dianion in  $\text{Na}_2(44\text{bipy})(\text{en})_2$  (**3**), allowing for interesting correlations to be drawn between electronic structure and metric structural data. Further characterization of the solids by means of powder X-ray diffraction, electron paramagnetic resonance, and/or elemental analysis is also reported.

Early electron paramagnetic resonance (EPR) studies on organic radicals in solution first identified the 4,4'-bipyridyl radical ( $44\text{bipy}^{\cdot}$ ) as a product of the reduction of pyridine with alkali metals.<sup>1</sup> Further confirmation of the existence of the radical was later corroborated by several other research groups employing both spectroscopic and electrochemical measurements, which yielded valuable information on the redox behavior of this species in solution.<sup>2,3</sup> More recently, studies employing a combination of ab initio theoretical methods and spectroscopic Raman measurements have also helped shine light on the structure and electronic properties of this highly reductive species.<sup>4</sup> However, despite these findings, no structural information on the radical anion is available beyond that obtained by means of the aforementioned computational studies. Similarly, to our knowledge, no report detailing the observation of the 4,4'-bipyridyl dianion has previously been made despite the fact that electrochemical studies of *N,N*-dimethylformamide solutions of 4,4'-bipyridine reveal two accessible consecutive reductions.<sup>2b,3</sup>

Our interest in such anionic species arose when it was

\* To whom correspondence should be addressed. E-mail: jose.goicoechea@chem.ox.ac.uk.

- (1) Carrington, A.; dos Santos-Veiga, J. *Mol. Phys.* **1962**, *5*, 21.
- (2) (a) Braterman, P. S.; Song, J.-I. *J. Org. Chem.* **1991**, *56*, 4678. (b) Kalyanaraman, V.; Rao, C. N. R. *J. Chem. Soc. B* **1971**, 2406.
- (3) (a) Roullier, L.; Laviron, E. *Electrochim. Acta* **1978**, *23*, 773. (b) Brown, O. R.; Butterfield, R. J. *Electrochim. Acta* **1982**, *27*, 321.
- (4) (a) Ould-Moussa, L.; Poizat, O.; Castella-Ventura, M.; Buntinx, G.; Kassab, E. *J. Phys. Chem.* **1996**, *100*, 2072. (b) Castella-Ventura, M.; Kassab, E. *J. Raman Spectrosc.* **1998**, *29*, 511. (c) Kihara, H.; Gondo, Y. *J. Raman Spectrosc.* **1986**, *17*, 263.

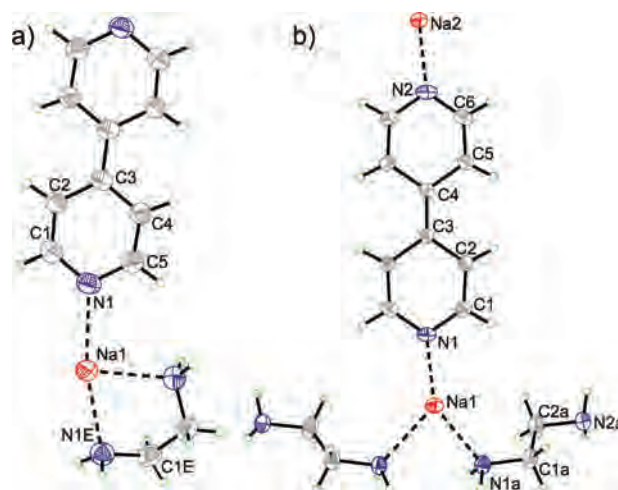


**Figure 1.** ORTEP representations of the repeating structural motifs in (a) **1** and (b) **3**. Anisotropic thermal ellipsoids pictured at 50% occupancy. Only the crystallographically unique non-hydrogen atoms are labeled.

observed that the radical anion could be synthesized as a reaction side product from the reduction of pyridine by solvated electrons present in solutions of deltahedral Zintl ions.<sup>5</sup> This observation prompted us to devise a synthetic route toward bulk quantities of the radical and to attempt a further reduction of this species to yield the dianion.

The reaction of 1 equiv of sodium metal with 44bipy in ethylenediamine (en) yielded an intensely colored purple solution from which we were able to isolate dark-purple air- and moisture-sensitive crystals of  $\text{Na}(44\text{bipy})(\text{en})$  (**1**), pictured in Figure 1a.<sup>6,7</sup> In addition to this species, we have also occasionally observed crystals of a compositionally identical crystalline phase,  $\text{Na}_2(44\text{bipy})_2(\text{en})_2$  (**2**), as a minor side product.<sup>7</sup> Powder X-ray diffraction studies on bulk samples of the radical anion demonstrate that **1** is the predominant crystalline phase and that **2** is only an occasional side product, often not observed in powder measurements (see the Supporting Information).

When a similar reaction was carried out employing a large stoichiometric excess of sodium metal (greater than 2 equiv),

(5) Goicoechea, J. M.; Hull, M. K.; Sevov, S. C. *J. Am. Chem. Soc.* **2007**, *129*, 7885.

the previously unobserved extremely air-sensitive dianion, 44bipy<sup>2-</sup>, was isolated alongside trace amounts of **1**.<sup>8</sup> This highly reduced organic anion has been characterized by single-crystal X-ray diffraction in the sodium salt Na<sub>2</sub>(44bipy)(en)<sub>2</sub> (**3**; Figure 1b).

Species **1** displays one-dimensional zigzag chains of sodium cations bridged by 4,4'-bipyridyl radicals. Each sodium ion (Na1) exhibits pseudo-square-planar coordination and is bound to a chelating en and to two radical anions [ $d_{\text{Na1-N1E}} = 2.506(2) \text{ \AA}$ ;  $d_{\text{Na1-N1}} = 2.426(1) \text{ \AA}$ ]. Interactions between chains arise in one dimension because of weak contacts between sodium ions and the  $\pi$  manifolds of bipyridyl linkers present in chains situated above and below the square plane [ $d_{\text{Na1-C4}} = 3.042(2) \text{ \AA}$ ]. The bond distances within the radical heterocycle are best discussed together with those of the dianion and are reviewed in detail below. EPR measurements on a solid sample of **1** showed a strong resonance arising from the unpaired electrons of the radical anions ( $g = 2.00429$ ; see the Supporting Information).

The compositionally identical crystalline phase, **2**, exhibits a three-dimensional (3D) structure where one of the crystallographically distinct sodium cations (Na1) is tetrahedrally coordinated by four 44bipy<sup>-</sup> spacers, generating a negatively charged 3D distorted diamondoid network [ $\text{Na-N}$  distances range between 2.359(1) and 2.392(2)  $\text{\AA}$ ]. Such diamondoid networks are ubiquitous in the chemistry of coordination solids and have been previously observed for neutral 4,4'-

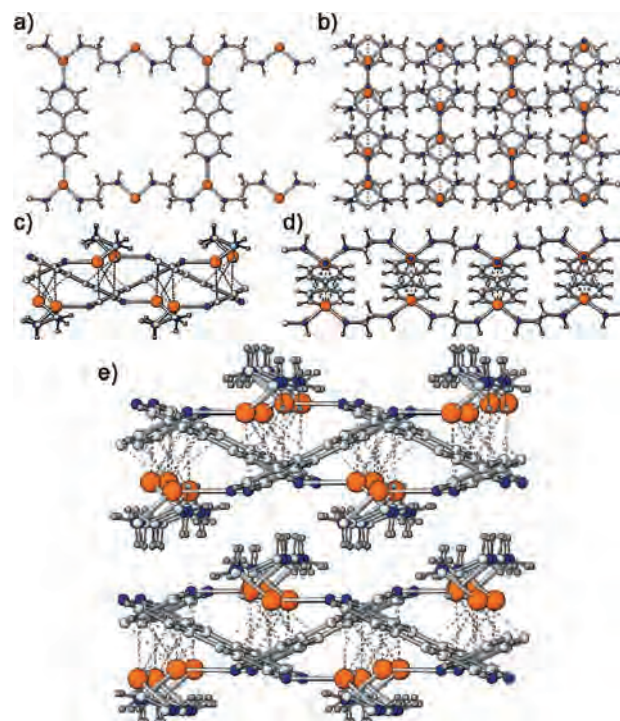


**Figure 2.** Bonding in **3**. (a) Representation of one of the three 2D networks involved in bonding. (b) Three networks that interweave, giving rise to a layer (pictured along the  $a$  axis); (c) view of the layer along the  $b$  axis and (d) view of layer along the  $c$  axis. (e) Representation of two 2D layers in the lattice.

(6) All operations were carried out under an inert atmosphere using standard Schlenk-line or glovebox techniques. In a typical experiment, 4,4'-bipyridine (0.150 g, 0.96 mmol) and sodium metal (0.024 g, 1.04 mmol) were weighed out into a test tube inside a nitrogen-filled glovebox ( $\text{H}_2\text{O} < 0.1 \text{ ppm}$ ;  $\text{O}_2 < 0.1 \text{ ppm}$ ). The solids were dissolved in approximately 5 mL of dry en, which immediately yielded a dark-purple solution. The mixture was allowed to stir overnight and subsequently filtered into a clean ampule. The purple solution was concentrated in vacuo on a Schlenk-line until half of the solvent had been removed. This solution was layered with benzene, yielding dark-purple blocklike crystals suitable for single-crystal X-ray diffraction after approximately 24 h (73% crystalline yield). Anal. Calcd for C<sub>12</sub>H<sub>16</sub>N<sub>4</sub>Na: C, 60.24; H, 6.74; N, 23.41. Found: C, 60.12; H, 6.71; N, 23.36.

(7) All single-crystal X-ray diffraction data were collected on an Enraf-Nonius Kappa-CCD diffractometer equipped with an Oxford Cryo-systems low-temperature device. Crystals were mounted on a glass fiber using N-Paratone oil and quickly placed under the nitrogen flow of the cryostream. Data were collected using graphite-monochromated Mo K $\alpha$  radiation; equivalent reflections were merged, and the images were processed with the *DENZO* and *SCALEPACK* programs. Corrections for Lorentz-polarization effects and absorption were performed, and the structures were solved by direct methods using *SHELXS*. The structures were refined on  $F^2$  using *SHELXL*. Crystal data for Na(bipy)(en) (**1**): monoclinic,  $C2/c$ ;  $a = 13.4043(4) \text{ \AA}$ ,  $b = 9.7710(4) \text{ \AA}$ ,  $c = 10.3943(4) \text{ \AA}$ ,  $\beta = 109.618(2)^\circ$ ;  $V = 1282.4(8) \text{ \AA}^3$ ;  $Z = 4$ ;  $T = 150(2) \text{ K}$ ;  $R1 = 0.043$ ,  $wR2 = 0.108$  [ $I > 2\sigma(I)$ ];  $R1 = 0.068$ ,  $wR2 = 0.119$  (all data). Crystal data for Na<sub>2</sub>(bipy)<sub>2</sub>(en)<sub>2</sub> (**2**): monoclinic,  $P2_1/c$ ;  $a = 9.7528(1) \text{ \AA}$ ,  $b = 16.1943(2) \text{ \AA}$ ,  $c = 17.2751(3) \text{ \AA}$ ,  $\beta = 104.7626(6)^\circ$ ;  $V = 2638.63(6) \text{ \AA}^3$ ;  $Z = 4$ ;  $T = 150(2) \text{ K}$ ;  $R1 = 0.044$ ,  $wR2 = 0.113$  [ $I > 2\sigma(I)$ ];  $R1 = 0.061$ ,  $wR2 = 0.124$  (all data). Crystal data for Na<sub>2</sub>(bipy)(en)<sub>2</sub> (**3**): orthorhombic,  $Pnma$ ;  $a = 15.1844(4) \text{ \AA}$ ,  $b = 13.0770(3) \text{ \AA}$ ,  $c = 8.3457(2) \text{ \AA}$ ;  $V = 1657.18(7) \text{ \AA}^3$ ;  $Z = 8$ ;  $T = 150(2) \text{ K}$ ;  $R1 = 0.043$ ,  $wR2 = 0.117$  [ $I > 2\sigma(I)$ ];  $R1 = 0.057$ ,  $wR2 = 0.127$  (all data). Crystal data for Na<sub>2</sub>(bipy)(en)<sub>2</sub> (**4**): orthorhombic,  $Cmca$ ;  $a = 13.2652(7) \text{ \AA}$ ,  $b = 15.2401(8) \text{ \AA}$ ,  $c = 8.3637(5) \text{ \AA}$ ;  $V = 1690.8(2) \text{ \AA}^3$ ;  $Z = 8$ ;  $T = 250(2) \text{ K}$ ;  $R1 = 0.069$ ,  $wR2 = 0.195$  [ $I > 2\sigma(I)$ ];  $R1 = 0.087$ ,  $wR2 = 0.207$  (all data).

(8) Procedure analogous to that described in ref 4. Sodium metal (0.055 g, 2.39 mmol) and 4,4'-bipyridine (0.150 g, 0.96 mmol) yielded dark-purple platelike crystals of Na<sub>2</sub>(bipy)(en)<sub>2</sub> from en/benzene (51% crystalline yield). Anal. Calcd for C<sub>7</sub>H<sub>12</sub>N<sub>3</sub>Na: C, 52.16; H, 7.50; N, 26.07. Found: C, 52.07; H, 7.53; N, 26.03.

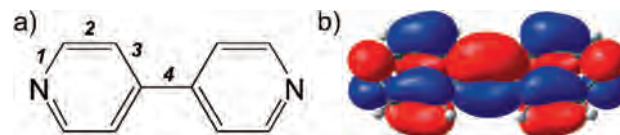


**Figure 3.** (a) Numbering scheme employed to discuss metric bond data for all of the 4,4'-bipyridine-derived species. (b) 4,4'-Bipyridine LUMO.

bipyridine and a range of metal cations.<sup>9</sup> However, all such networks tend to be positively charged, with charge-balancing anions occupying the pores left in the network structure. Inversely, the voids within **2** are occupied by [Na(en)<sub>2</sub>]<sup>+</sup> cations, which also appear to interact to some degree with adjacent bipyridyl  $\pi$  systems [closest contact: 3.026(2)  $\text{\AA}$ ].

Solid **3** exhibits a layered structure comprised of two-dimensional (2D) sheets. Each 4,4'-bipyridyl dianion acts as a bridge between two crystallographically distinct sodium ions [ $d_{\text{Na1-N1}} = 2.360(2) \text{ \AA}$ ;  $d_{\text{Na2-N2}} = 2.372(2) \text{ \AA}$ ]. These subunits form an undulating 2D net by means of en molecules, which interlink sodium centers [ $d_{\text{Na1-N1A}} = 2.462(2) \text{ \AA}$ ;  $d_{\text{Na2-N2A}} = 2.472(1) \text{ \AA}$ ], giving rise to an extended 2D network, as pictured in Figure 2a. In turn, three such nets interweave, giving rise to a tightly packed layer (Figure 2b–d) exhibiting interactions between sodium ions and the  $\pi$  systems of adjacent bipyridyl spacers [ $d_{\text{Na1-C4}} = 2.822(2) \text{ \AA}$ ;  $d_{\text{Na1-C5}} = 2.879(2) \text{ \AA}$ ;  $d_{\text{Na1-C6}} = 3.050(2) \text{ \AA}$ ;  $d_{\text{Na2-C1}} = 3.071(2) \text{ \AA}$ ;  $d_{\text{Na2-C2}} = 2.873(2) \text{ \AA}$ ;  $d_{\text{Na2-C3}} = 2.801(2) \text{ \AA}$ ]. These values are comparable to other reported interactions

(9) For an overview of 4,4'-bipyridine in modular networks, see: Yaghi, O. M.; Li, H.; Davis, C.; Richardson, D.; Groy, T. L. *Acc. Chem. Res.* **1998**, *31*, 474, and references cited therein.

**Table 1.** Bond Lengths [Å] for 4,4'-Bipyridine and the 44bipy<sup>•-</sup> and 44bipy<sup>2-</sup> Moieties in Species 1–4

bond <sup>a</sup>	4,4'-bipy <sup>b</sup>	4,4'-bipy <sup>•-</sup>				4,4'-bipy <sup>2-</sup>	
		Na(44bipy)(en) (1)	Na <sub>2</sub> (44bipy) <sub>2</sub> (en) <sub>2</sub> (2)		Na <sub>2</sub> (44bipy)(en) <sub>2</sub> (3)	Na <sub>2</sub> (44bipy)(en) <sub>2</sub> (4)	
1	1.336	1.354(2) 1.360(2)	1.353(2) 1.355(2) 1.359(2)	1.352(2) 1.353(2)	1.352(2) 1.356(2)	1.378(2) 1.378(2)	1.369(4)
2	1.383	1.364(2) 1.371(2)	1.366(2) 1.367(2) 1.368(2) 1.368(2)	1.371(2) 1.371(2)	1.364(2) 1.365(2)	1.364(2) 1.365(2)	1.359(4)
3	1.390	1.423(2) 1.430(2)	1.422(2) 1.423(2) 1.424(2) 1.426(2)	1.425(2) 1.427(2)	1.423(2) 1.425(2)	1.463(2) 1.467(2)	1.460(4)
4	1.484	1.424(3)	1.427(2)	1.423(3)	1.427(3)	1.383(3)	1.384(8)

<sup>a</sup> Bond numbering scheme, as indicated in Figure 3a. <sup>b</sup> Mean metric bond data taken from a survey of the 1965 crystallographically characterized species containing 4,4'-bipyridine reported in the Cambridge Structural Database at the time of preparation of this manuscript.

between sodium ions and neutral aryl-ring-based moieties.<sup>10</sup> Further stacking of the layers is present in the lattice with no apparent interactions between them (Figure 2e).

Interestingly, solid **3** was found to undergo a phase transition from the primitive orthorhombic space group *Pnma* to its minimal nonisomorphic supergroup *Cmca* (**4**) between 200 and 250 K.<sup>7</sup> The principal difference observed between phases is that while in *Pnma*, there are two crystallographically distinct sodium ions (Na1 and Na2), these become equivalent upon transition to *Cmca*. This has an effect on the distances between sodium ions and coordinated nitrogen atoms [ $d_{\text{Na1-N1}} = 2.363(4)$  Å;  $d_{\text{Na1-N1A}} = 2.471(3)$  Å] as well as between sodium ions and adjacent 44bipy<sup>2-</sup> dianions [ $d_{\text{Na1-C1}} = 3.046(4)$  Å;  $d_{\text{Na1-C2}} = 2.886(4)$  Å;  $d_{\text{Na1-C3}} = 2.826(4)$  Å].

Bond distances within each of the 4,4'-bipyridyl-derived anions (44bipy<sup>•-</sup> and 44bipy<sup>2-</sup>) can be directly correlated to the electronic structure of the neutral parent compound. Ab initio computational studies on 44bipy reveal an accessible singly degenerate LUMO comprised of  $\pi$ -orbital contributions from all of the heterocyclic atoms (Figure 3b).<sup>11</sup> Further inspection of this orbital reveals bonding and antibonding interactions between element pairs and subsequently upon reduction (occupation of the LUMO), and one would expect these bonds to shorten or elongate, respectively. Additional calculations on 44bipy<sup>•-</sup> and 44bipy<sup>2-</sup> reveal orbitals identical with a SOMO and a HOMO, respectively.

The stepwise reduction of 4,4' bipyridine to yield 44bipy<sup>•-</sup> and 44bipy<sup>2-</sup> results in an elongation of bond 1 due to the antibonding character of this bond in the LUMO. We have observed that bond 1 lengthens from 1.336(av) Å for neutral 4,4'-bipyridine to averages of 1.355 Å for 44bipy<sup>•-</sup> and 1.375 Å for 44bipy<sup>2-</sup> (comprehensive bond data are presented in Table 1). A similar trend is observed for bond 3 (also antibonding): 1.390 Å (av) for 44bipy, 1.425 Å (av) for 44bipy<sup>•-</sup>, and 1.463 Å (av) for 44bipy<sup>2-</sup>. Conversely, bonds

2 and 4 follow an inverse trend, shortening upon reduction. Thus, bond 2 contracts from 1.383 Å (av) for 44bipy to 1.368 Å (av) for 44bipy<sup>•-</sup> and 1.363 Å (av) for bipy<sup>2-</sup>. Finally, bond 4 undergoes the most dramatic variation (from a single to a double bond), shrinking from 1.484 Å (av) for 44bipy to av 1.425 Å (av) for 44bipy<sup>•-</sup> and 1.384 Å (av) for 44bipy<sup>2-</sup>.

Further structural repercussions due to the reduction of the neutral parent precursor are evident in the torsion angle between the two pyridyl rings of the bipyridyl moieties in each of the reduced species. These values range between 0.0° and 3.2(1)° for compounds **1–4** because of the greater degree of  $\pi$  overlap present in the bonds linking pyridyl rings. These values are notably smaller than the predicted theoretical value of 40.8° reported in the literature for 4,4'-bipyridine.<sup>12</sup> Similarly, a survey of all of the crystallographically characterized solids containing 4,4'-bipyridine reveals a mean value of 18° for the torsion angle between heterocyclic rings, also substantially larger than the values observed for **1–4**, albeit influenced by additional factors such as lattice effects.

The reported research highlights results of ongoing studies investigating the reduction of heterocyclic organic ligands with the aim of employing their anionic doppelgangers in metal–organic frameworks.

**Acknowledgment.** We thank the EPSRC (EP/F00186X; PDRA funding for M.S.D.) and the University of Oxford for financial support. We also thank Steve Boyer (London Metropolitan University) for elemental analyses and the University of Oxford for access to CAESR, OSC, and Chemical Crystallography facilities.

**Supporting Information Available:** X-ray crystallographic file in CIF format (**1–4**), thermal ellipsoid plot of **2**, PXRD data, EPR spectra of **1**, full ref 11, and table of bond metrics for computationally optimized geometries. This material is available free of charge via the Internet at <http://pubs.acs.org>. IC800726P

(10) For example, see: Bock, H.; Ruppert, K.; Havlas, Z.; Fenske, D. *Angew. Chem., Int. Ed.* **1990**, *29*, 1042.

(11) DFT calculations performed using B3LYP/3-21+G\* and the *Gaussian03* package: Frisch, M. J. *Gaussian03*, revision D.01; Gaussian Inc.: Wallingford, CT, 2004.

(12) Barone, V.; Lelj, F.; Comisso, L.; Russo, N.; Cauletti, C.; Piancastelli, M. N. *Mol. Phys.* **1983**, *49*, 599.